

The stabilizing effects of axial stretching on turbulent vortex dynamics

David S. Nolan

Department of Atmospheric Science, Colorado State University, Fort Collins, Colorado 80523

(Received 18 October 2000; accepted 16 March 2001)

The evolution and dynamics of vortices in inviscid, incompressible flow under the influence of a deformation field which causes stretching in the axial direction are studied. These vortices are simulated using three-dimensional vortex methods which offer the advantages of having no inherent numerical dissipation and great computational efficiency for short to intermediate times. Two cases in particular are studied: The evolution of a stable, but strongly perturbed vortex, and the evolution of an unstable vortex. In both types of vortices, it is found that the stretching and radial inflow associated with the surrounding deformation field can suppress the growth of disturbances and slow the development of turbulence. This stabilization is even greater than what one would expect from the purely kinematic effects of the deformation field alone, indicating there is a negative feedback on the nonlinear vortex dynamics. The physical mechanisms for stabilization by stretching are discussed, along with potential applications for understanding the stability of intense geophysical vortices maintained by convection. © 2001 American Institute of Physics.
[DOI: 10.1063/1.1370390]

I. INTRODUCTION

Intense vortices are the common feature among a variety of severe weather phenomena, such as tornadoes, mesocyclones (supercells), and hurricanes. The very high vorticity at the core of these phenomena is generated by the stretching of vertical vorticity. In strong tornadoes and thunderstorms, this vertical vorticity is believed to come from the tilting of horizontal vorticity associated with the shear of the environmental flow.^{1,2} In hurricanes, it is the planetary vorticity which is amplified.³ For all three cases, it is intense convection (driven by the release of latent heat from condensation) that forces convergence at low levels and creates the deformation field which stretches and intensifies the local vertical vorticity.

The literature on the stability of geophysical vortices is vast. However, only a small fraction of this literature takes into consideration the deformation field surrounding the vortex which creates and sustains it. Rather, the effects of deformation on vortices and their stability have been studied extensively in the context of understanding the fine-scale structure of vortices in turbulent shear flows. The early work of Moore and Saffman⁴ and Tsai and Widnall⁵ established that a three-dimensional vortex which is deformed into an elliptical shape by a planar straining field will then be susceptible to three-dimensional instabilities (aka the TWMS instability). These and other earlier papers, such as that of Robinson and Saffman,⁶ treated vortices whose cores consisted of a finite region of constant vorticity, which are elliptical in the presence of strain and circular otherwise. The TWMS instability is a “large-scale” instability, as it is a stationary amplifying disturbance of azimuthal wave number one with axial wavelengths comparable to the core diameter. An additional class of instabilities in strained vortices was discovered by Pierrehumbert,⁷ which are of small scales and are associated with the elliptical nature of the streamlines in

the cores of these vortices. These smaller-scale instabilities have been shown by Landman and Saffman⁸ to persist in the presence of viscosity and, in the inviscid case, were supported with analytic solutions by Waleffe.⁹

The preceding analyses considered only vortices subjected to planar strain perpendicular to the principal vortex axis. For viscous fluids, a vortex subjected to purely axisymmetric stretching will evolve to a steady state, the famous Burgers vortex,¹⁰ whose core vorticity distribution is Gaussian. In the presence of an additional planar strain, these vortices will also become elliptical, as was shown in the low-Reynolds number limit by Robinson and Saffman¹¹ and then for higher Reynolds numbers by Moffat, Kida, and Ohkitani¹² and by Prochazka and Pullin¹³ (for problems of this type the Reynolds number is typically defined as Γ/ν , where Γ is the vortex circulation and ν is the kinematic viscosity). These studies found that both symmetric and elliptical (due to straining) Burgers-type vortices are stable to purely two-dimensional (asymmetric) disturbances. For symmetric Burgers vortices, Nolan and Farrell¹⁴ found that the radial inflow associated with the stretching field also decreases the maximum possible *transient* growth of optimally configured initial perturbations, due to the fact that the radial inflow advects the perturbations through the region of maximum shear, which is where the largest transient growth can occur.

However, the existence of three-dimensional instabilities in nonstretched, strained vortices raises the specter of three-dimensional instabilities in vortices that are both stretched and strained. Nonetheless, the stabilizing effects of the stretching field have been shown to be effective on three-dimensional perturbations by Le Dizès, Rossi, and Moffat¹⁵ for unsteady, stretched and strained vortices and by Eloy and Le Dizès¹⁶ for steady, stretched and strained vortices, provided the stretching is sufficiently large compared to the

strain. The effect of the deformation (stretching) field is to continuously change the structure and wave number of the perturbations, such that they cannot remain in the spectrum of unstable wave numbers associated with the small-scale instabilities.

Not surprisingly, the fully nonlinear dynamics of perturbations to stretched vortices have not received nearly as much attention. Neu¹⁷ found asymptotic equations that describe the collapse of a perturbed Burgers' vortex sheet into circular vortices; when the deformation that sustains the sheet is strong enough, this collapse is prevented. Using asymptotic equations which describe the nonlinear evolution of slender vortex filaments, Klein, Majda, and McLaughlin¹⁸ showed that sufficient stretching along the axis of slender vortex filament can guarantee its nonlinear stability, provided this stretching is large enough compared to the rate of deformation in the orthogonal directions. The common result among these studies is that convergence and stretching have a stabilizing effect.

Of course, in geophysical contexts, whether or not the deformation is strong enough to play a role in stability should be considered on a case by case basis. Nonetheless, it is certainly worthwhile to consider the effects of stretching on vortex stability. Previous studies such as those outlined above have been restricted to either linearized dynamics or very idealized vortices. Here we present numerical simulations which indicate that this stabilizing effect extends to the fully nonlinear dynamics of more general vortices. These simulations use three-dimensional vortex methods to integrate the Euler equations forward in time. We demonstrate the transition to turbulence in a stable, but strongly perturbed vortex, and in an unstable vortex, and then show how this transition is slowed under the effects of axial stretching.

It should be noted that a wide variety of issues concerning the stability and behavior of three-dimensional vortices might be addressed with the method and the numerical model presented here. While we will touch on some of these issues, a full assessment of three-dimensional inviscid vortex dynamics is beyond the scope of this paper, and we will instead focus on the dynamics of stretched, symmetric vortices. In Sec. II we briefly describe three-dimensional vortex methods. In Sec. III, the two types of vortices and the deformation field which causes axial stretching are presented. Sections IV and V show the results of simulations with and without axial stretching for the two vortices. The reasons for stabilization by stretching are discussed in Sec. VI, and conclusions are drawn in Sec. VII.

II. VORTEX METHODS FOR INCOMPRESSIBLE, INVISCID FLOW IN THREE DIMENSIONS

In two dimensions, vortex methods simulate the evolution of incompressible fluid flow by computing the trajectories of localized vortices in the plane.¹⁹⁻²¹ Since the vorticity is conserved in two-dimensional flows, the vortex strengths do not change in time. An important result from research on the convergence of vortex methods is that their results are much more accurate when the vorticity associated with each element is smooth, i.e., "blob" methods are much more ac-

curate than "point" methods. In fact, the rate of convergence depends very strongly on the distribution of the vorticity within the blob.²²⁻²⁵

Extending these ideas to three dimensions,²⁶⁻²⁸ we represent the vorticity field with a collection of vortex tubes, each of which has a vorticity distribution in its core which is smooth and has a finite "cut-off" radius. The center axis of each vortex tube is represented by a continuous chain of segments, each of which is the straight line between its two endpoints \mathbf{x}_j and \mathbf{x}_{j+1} . The familiar concepts that vortex lines are material curves and must not end in the fluid require that the endpoints move with the flow and that individual vortex tubes remain connected at all times.

For a smooth vorticity field $\omega(\mathbf{x})$ in an unbounded domain, a vector potential ϕ may be found with the use of the Green's function for the Laplace equation

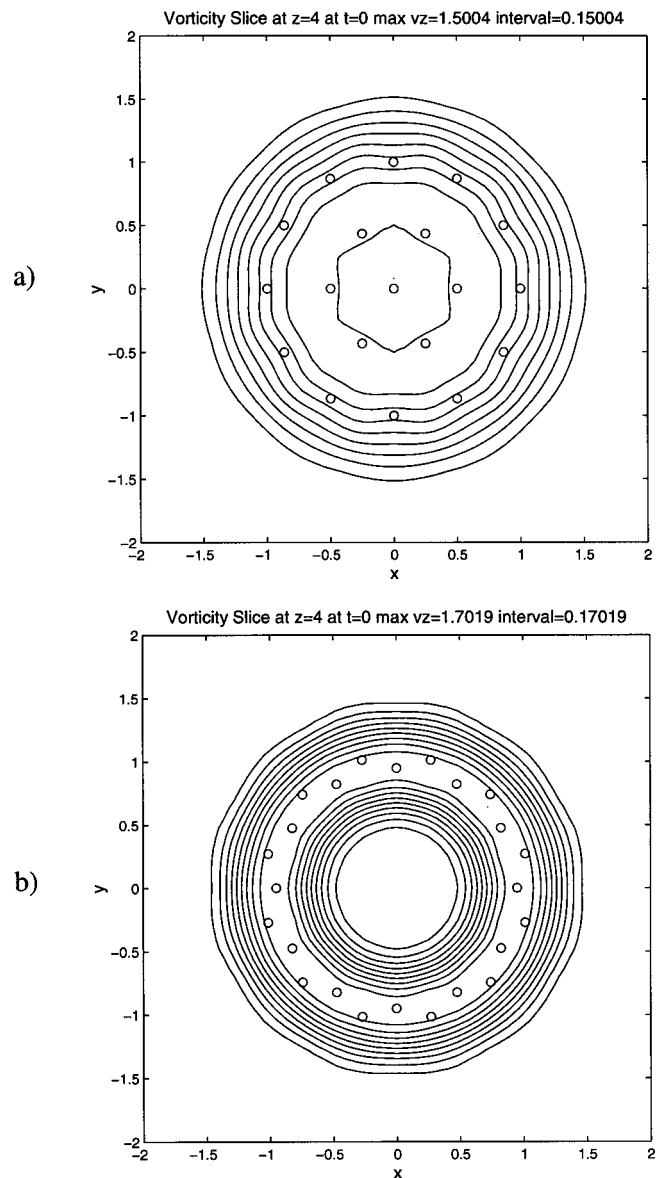


FIG. 1. Vertical vorticity contours and the locations of the centers of the vortex lines for (a) the stable vortex; (b) the unstable vortex.

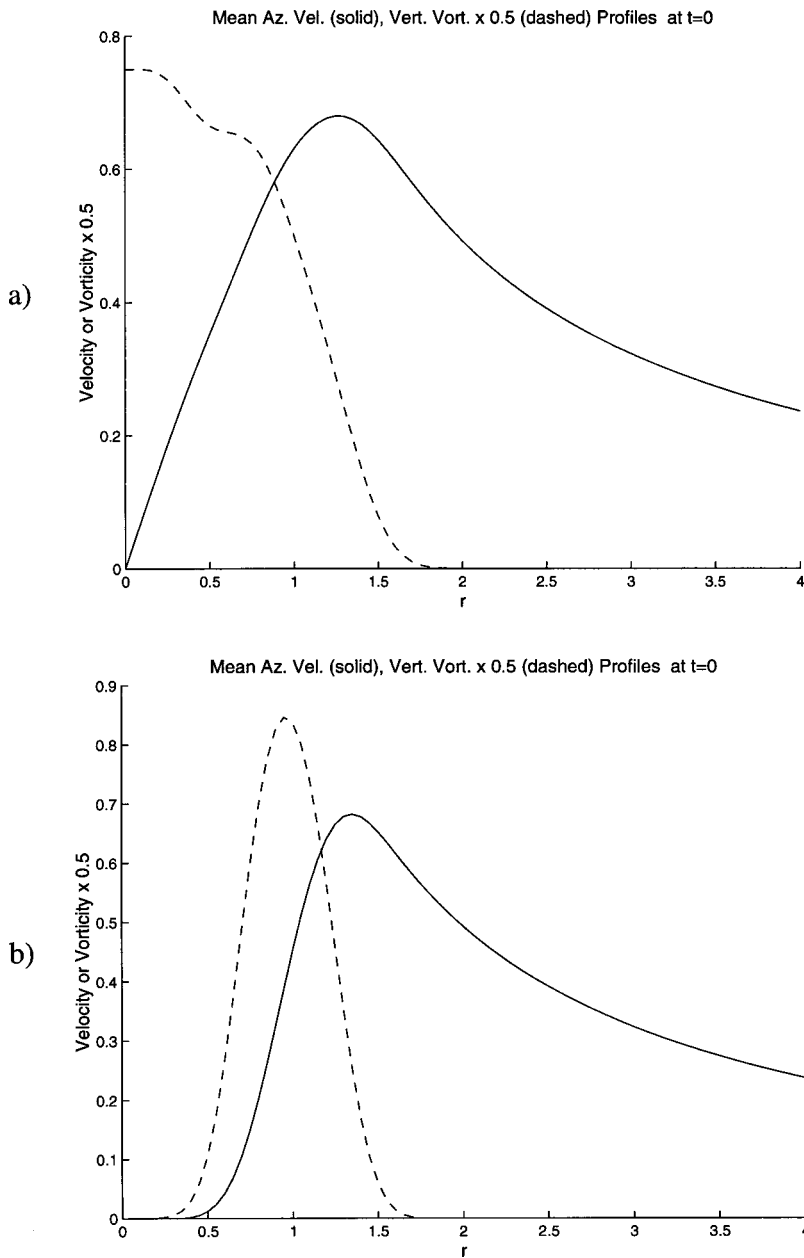


FIG. 2. Radial profiles of azimuthal velocity (solid) and vertical vorticity (dashed) for (a) the stable vortex; (b) the unstable vortex.

$$\phi(\mathbf{x}) = \int_{R^3} \frac{\omega(\mathbf{x}')}{4\pi|\mathbf{x}-\mathbf{x}'|} d\mathbf{x}', \tag{1}$$

with the associated velocity field

$$\mathbf{u}(\mathbf{x}) = \nabla \times \phi = - \int_{R^3} \frac{(\mathbf{x}-\mathbf{x}') \times \omega(\mathbf{x}')}{4\pi|\mathbf{x}-\mathbf{x}'|^3} d\mathbf{x}'. \tag{2}$$

In the practice of vortex methods, (2) is replaced by a summation over all the vortex segments of all the tubes, with the incorporation of a smoothing function $f(r)$ which is related to the vorticity distribution $g(r)$ in the core of the vortex tube by $f'(r) = 4\pi r^2 g(r)$. The velocity field may then be written

$$\mathbf{u}(\mathbf{x}, t) = - \frac{1}{4\pi} \sum_j \Gamma_j \frac{(\mathbf{x}_j^c - \mathbf{x}) \times (\Delta \mathbf{x}_j)}{|\mathbf{x}_j^c - \mathbf{x}|^3} f\left(\frac{|\mathbf{x}_j^c - \mathbf{x}|}{\delta}\right), \tag{3}$$

where Γ_j is the circulation (strength) of each segment (constant for each individual filament), \mathbf{x}_j^c is the midpoint of each segment, $\Delta \mathbf{x}_j$ is the vector connecting its endpoints, and δ is the cut-off radius of the internal vorticity distribution. The simulations presented here use

$$f(r) = 1 - e^{-r^3}, \tag{4}$$

and its associated vorticity core function

$$g(r) = \frac{3}{4\pi} e^{-r^3}, \tag{5}$$

which are known to allow for second-order convergence.^{23,29,30} The evolution of the vortex lines is described by the system

$$\frac{d\mathbf{x}_j}{dt} = \mathbf{u}(\mathbf{x}_j, t), \tag{6}$$

which we integrate in time with a fourth order Runge–Kutta scheme. As the vortex lines evolve, they will (usually) stretch and the segments will become longer. To achieve accuracy in the self-induced motion of curved vortex lines, it is critical that the lengths of the segments remain considerably smaller than their cut-off radii.³¹ Thus, if a segment becomes longer than half its cut-off radius, we replace it with two segments by adding a new point in between its endpoints using a cubic interpolation scheme.

Perhaps the most common misunderstanding about vortex methods is the confusion between physical vortices and numerical vortex elements. Unlike a physical vortex, the cores of the vortex tubes described above do not change size or shape as they are advected by the flow. Rather, a physical vortex must be represented by a collection of numerical vortices, and accuracy is achieved with a high density of overlapping numerical vortices. The collective motions of these numerical elements will then properly represent the evolution of the smoothly varying vorticity field. Further discussion on these points^{20,27} and some applications similar to the problem investigated here are available.^{32,33}

III. INITIAL CONDITIONS AND DEFORMATION FIELD

In this paper we present results for two specific cases: A vortex with an initial internal vorticity profile which is stable, but is modified by a large-amplitude perturbation, and a vortex which is unstable, and modified only by very small amplitude perturbations. We study the evolution of both vortices under varying degrees of axial stretching. Below, the internal structure of these vortices and the deformation field which causes the axial stretching are described.

A. A stable, strongly perturbed vortex

As a simple representation of a stable vortex, we use 19 vortex lines arranged in concentric circles about a central axis, placing one line at the center, 6 lines equally spaced around the circle at $r=0.5$, and 12 lines equally spaced around the circle at $r=1.0$. This arrangement of vortex lines, and a cross section of the resulting vorticity field, is shown in Fig. 1(a). All segments have a cut-off radius $\delta=0.5$, thus ensuring substantial overlap among all the lines with their neighbors. The strengths of the lines are all equal, such that the total circulation equals 2π . Figure 2(a) shows radial profiles of the mean velocity and vorticity associated with this vortex. The flow is periodic in the vertical (z) direction with periodicity $L=8.0$. This periodicity is approximated with image vortices above and below the domain. While an exact computation of periodic flow would require either an infinite series of image vortices, or computation of the periodic Green function, this method is sufficiently accurate for our purposes.

For our large-amplitude perturbation, we displace the vortex lines in the x direction with a Gaussian of width 2.0 and a maximum amplitude of 1.5 at $z=4.0$. To break the symmetry of the initial perturbation, and to help the transition to three-dimensional dynamics, we also add to the x , y , and z positions of the vortex segment endpoints (the \mathbf{x}_j 's)

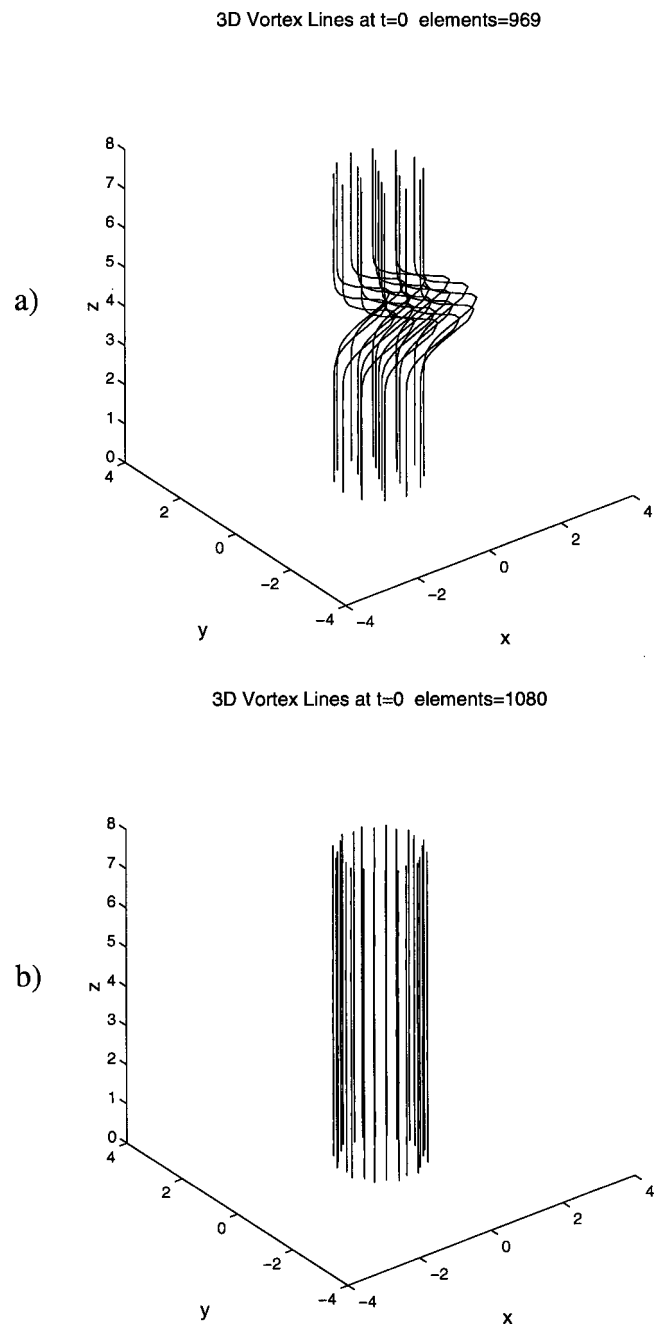


FIG. 3. Initial vortex line configurations for (a) the stable, strongly perturbed vortex; (b) the unstable, weakly perturbed vortex.

Gaussian random noise with variance 1.0×10^{-6} . This results in the initial condition shown in Fig. 3(a).

B. An unstable, weakly perturbed vortex

Our unstable vortex is represented by 24 vortex lines, 12 each arranged equally spaced around the circles at $r=0.95$ and $r=1.05$. The outer ring of lines is initially rotated so that the angular position of each outer line is exactly between the nearest inner lines, as shown with the vertical vorticity field in Fig. 1(b). The cut-off radii are $\delta=0.4$, so as to produce a narrow annulus of nonzero vorticity from $0.25 < r < 1.75$ as shown in Fig. 2(b). The initial periodicity is again $L=8.0$. To instigate three-dimensional instabilities, we again add ran-

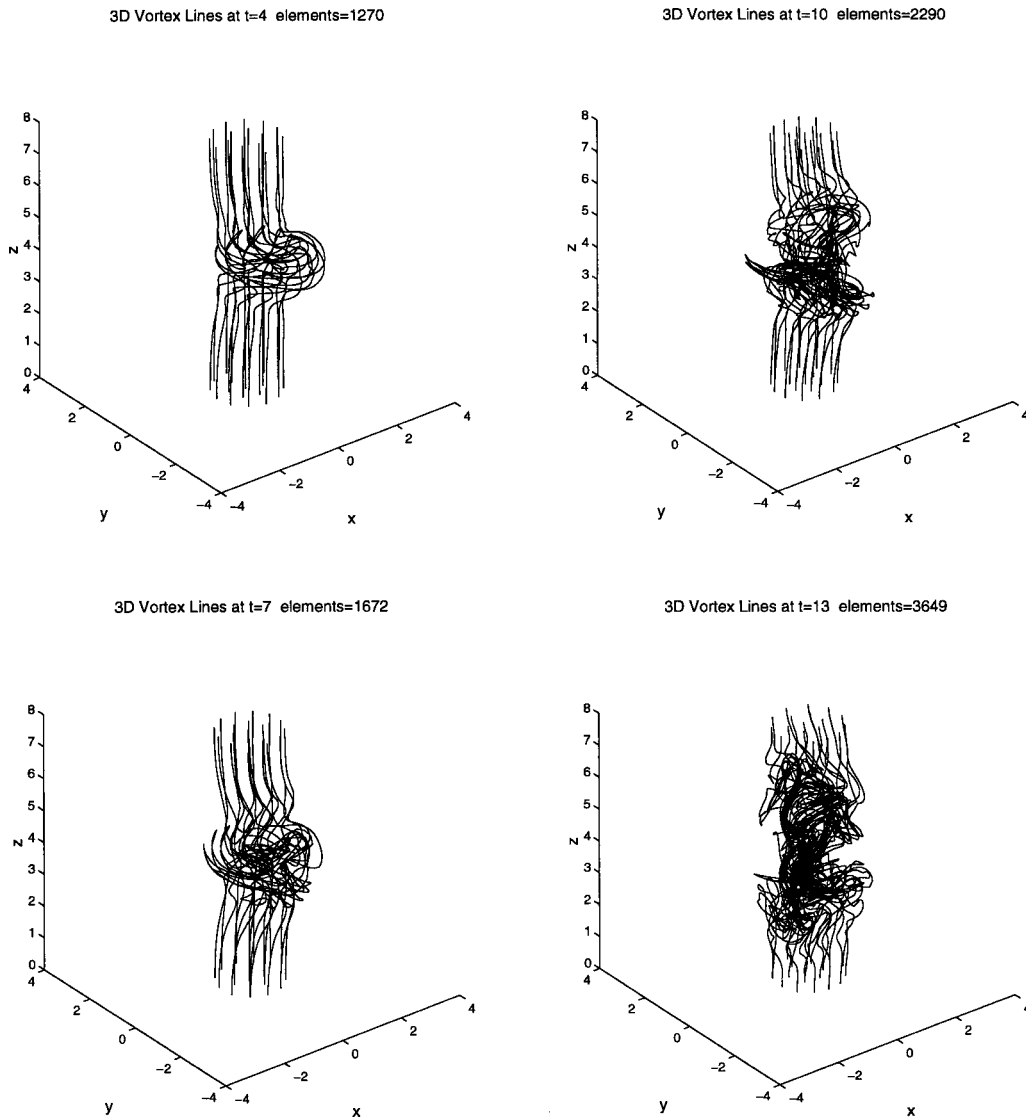


FIG. 4. Snapshots of the vortex lines for the stable, perturbed vortex at $t=4, 7, 10,$ and $13,$ without axial stretching ($c=0$).

dom noise to the initial locations of the segment endpoints with variance 1.0×10^{-6} . Figure 3(b) depicts the initial arrangement of the vortex lines for the unstable vortex.

C. An axisymmetric deformation field

In most of the simulations to follow, we add to the velocity field a background flow in the form of an unbounded cylindrical deformation field

$$U = -\frac{1}{2}cx, \quad V = -\frac{1}{2}cy, \quad W = cz, \quad (7)$$

where c is a positive constant. Since the background flow has zero vorticity, it is not changed by the vortex and remains constant in time.³⁴ Note that while the vortices are periodic in the z direction the deformation field (7) is unbounded; this is not inconsistent because the flow field has a rate of vertical stretching $\partial W/\partial z=c$ which is constant everywhere. As time evolves the vortices will be stretched in the vertical direction and thus their periodic length will also increase, i.e., L

$=L(t)=L_0e^{ct}$, where e^{ct} is the distance between any two particles in the deformation field initially one unit of distance apart in the vertical direction.

IV. EVOLUTION OF THE STABLE, PERTURBED VORTEX

We now consider the evolution of the stable, strongly perturbed vortex. The evolution of the vortex without deformation ($c=0.0$) is shown in Fig. 4. As time evolves, the Gaussian kink in the vortex lines is sheared by the differential rotation outside of the vortex core. This shearing causes the lines to strongly interact with themselves and their neighbors. These nonlinear interactions cause the core of the vortex to break down into three-dimensional turbulence, and the complexity of the vortex lines increases very rapidly. (For small amplitude perturbations, the kink propagates away from its initial location, both in the azimuthal and vertical directions, in the manner of vortex Kelvin waves.^{35,36} The

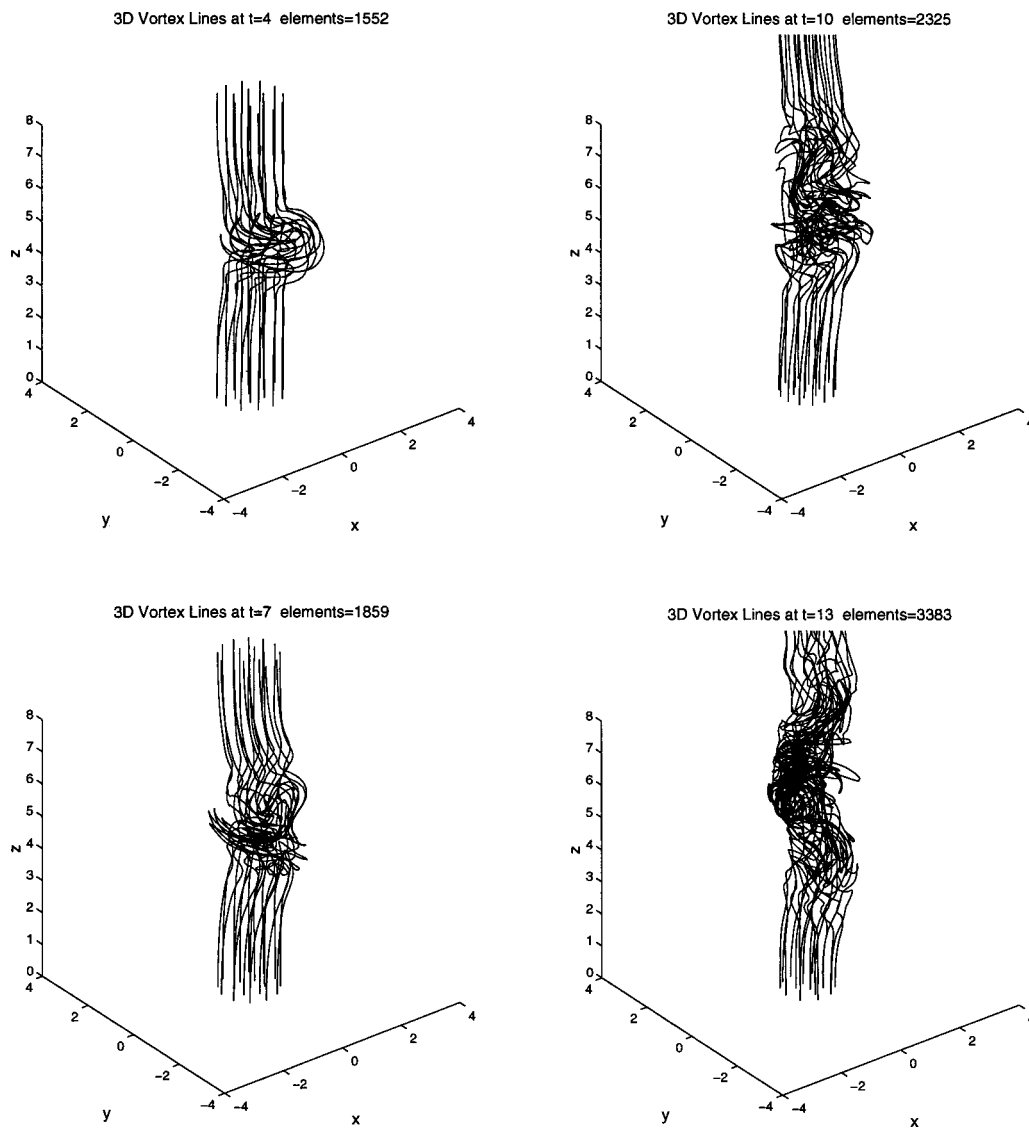


FIG. 5. Snapshots of the vortex lines for the stable, perturbed vortex at $t=4, 7, 10,$ and $13,$ with axial stretching ($c=0.04$).

amplitude of the initial perturbation has been chosen so that the dynamics become fully nonlinear in a short time.)

The evolution of the same vortex under axial stretching with $c=0.04$ is shown in Fig. 5. Note how the length of the vortex (and its associated periodicity) increases with time, and the initial disturbance is advected away from $z=4.0$. At each point in time, the turbulence in the vortex core is noticeably less developed for the vortex under axial stretching than for the vortex without stretching. For example, at $t=13$ in the vortex with $c=0.0$, the extensive vortex stretching and folding of the vortex lines (to the point where individual lines cannot be identified) is such that the vortex core no longer appears as a coherent vortex tube from $z=3$ to $z=6$. At $t=13$ in the stretched case, the vortex does appear to have gone considerable twisting and folding from $z=6$ to $z=8$, but the lines still represent a coherent vortex tube.

It is certainly evident that the axial stretching is slowing the development of three-dimensional turbulence in the core of the vortex. This is due in part to the fact that any horizontal vorticity, generated by the vortex dynamics, will be di-

minished over time by the horizontal compression associated with the deformation field. This will be shown explicitly below. Vertical vorticity, while amplified by the deformation field, only contributes to the intensity of the vortex already present. A natural question to ask is whether or not the turbulent development is slowed *even more* (or less) than what would be expected purely from the kinematic effects of the deformation field.

The total length of the vortex lines can be used as an approximate measure for the rate of growth of turbulence in the core of the vortex. We say approximate because the velocity and vorticity fields are not nearly as ‘‘rough’’ as the lines suggest, due to the substantial cancellation among the lines and their rather smooth vorticity cores.³⁷ As the vortices evolve, both real and numerical vortex lines are contorted, twisted, and stretched by nonlinear interactions with themselves and their with neighbors. For $c \neq 0$, the vortex lines are stretched in the vertical direction and compressed in the horizontal directions by the deformation field. Thus, we would like a measure of the total length of the vortex lines

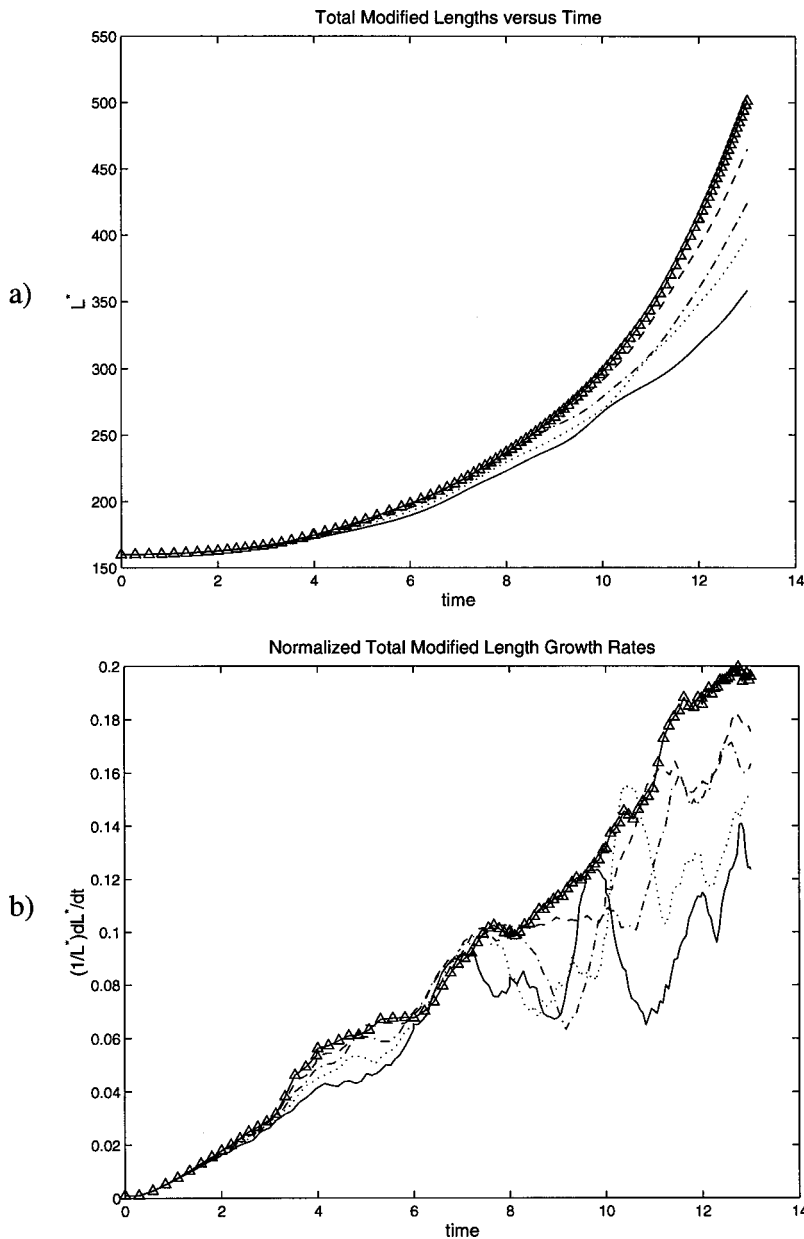


FIG. 6. Total modified lengths of the vortex lines (a), and their normalized growth rates (b), as a function of time for the stable, strongly perturbed vortex for various values of the deformation parameter c : Solid, $c=0.0$; dashed, $c=0.02$; dash-dot, $c=0.04$; dotted, $c=0.06$; solid, $c=0.08$.

which accounts for the effects of the deformation field, such that we can determine to what extent the nonlinear, vortex-vortex interactions are modified in the presence of axial stretching.

To construct such a measure, we first compute the total lengths of the vortex lines projected along each axis

$$L_x = \sum_{m=1}^M \sum_{n=1}^{N-1} |x_{m,n+1} - x_{m,n}|, \tag{8}$$

$$L_y = \sum_{m=1}^M \sum_{n=1}^{N-1} |y_{m,n+1} - y_{m,n}|, \tag{9}$$

$$L_z = \sum_{m=1}^M \sum_{n=1}^{N-1} |z_{m,n+1} - z_{m,n}|, \tag{10}$$

where the subscripts $m=1 \cdots M$, $n=1 \cdots N$ refer to the M vortex lines with N points each. At first thought, one may be tempted to simply divide the vertical length L_z by the expo-

ponential factor e^{ct} , which is the vertical distance between any two points initially a unit distance apart in the vertical at time $t=0$, and the horizontal lengths L_x and L_y by the factor $e^{-ct/2}$, for similar reasons [cf. Eq. (7)]. However, this would overestimate the effects of deformation, because any “new” vertical length generated by turbulent motions at later times in the vortex would be overly diminished by the stretching factor which increases exponentially from $t=0$ (rather than from the time that this new vertical length had been created), and similarly the horizontal lengths would be overly magnified. In the absence of any vortex dynamics (i.e., if we set the vortex line strengths to zero), the vertical vortex length would obey

$$\frac{dL_z}{dt} = cL_z, \tag{11}$$

while the horizontal line lengths would obey

$$\frac{dL_x}{dt} = -\frac{1}{2} cL_x, \tag{12}$$

$$\frac{dL_y}{dt} = -\frac{1}{2} cL_y. \tag{13}$$

Therefore, to eliminate the effects of the deformation on the total line length (as opposed to the effects of vortex dynamics), we compute modified vortex line lengths

$$L_x^*(t) = L_x(0) + \int_0^t \left(\frac{dL_x}{dt'} + \frac{1}{2} cL_x \right) dt', \tag{14}$$

$$L_y^*(t) = L_y(0) + \int_0^t \left(\frac{dL_y}{dt'} + \frac{1}{2} cL_y \right) dt', \tag{15}$$

$$L_z^*(t) = L_z(0) + \int_0^t \left(\frac{dL_z}{dt'} - cL_z \right) dt'. \tag{16}$$

These modified line lengths (14)–(16) are then combined to produce a *total modified vortex line length*

$$L^*(t) = \{L_x^*(t)^2 + L_y^*(t)^2 + L_z^*(t)^2\}^{1/2}. \tag{17}$$

We expect this measure to indicate the rate of development of turbulence in the vortex purely through the dynamics of the vorticity field itself. The modified lengths (17) are shown in Fig. 6(a) for simulations with $c = 0.0, 0.02, 0.04, 0.06,$ and 0.08 . For increasing stretching rates, the rate of growth of the lengths of the vortex lines is decreased. Also shown in Fig. 6(b) are the instantaneous growth rates of the total modified lengths, divided by the current total modified length at each instant, which is an approximate measure of the rate at which the vortex lines are being stretched by the turbulent vortex dynamics. These normalized growth rates also show that the turbulent development decreases with increasing stretching, although the growth rates are somewhat oscillatory, such that occasionally the growth rates for cases with larger stretching rates exceed those with smaller stretching rates.

A more direct way to view the development of disturbances is through examination of the vorticity fields generated by the vortex lines. Since the vertical vorticity field is dominated by the mostly axisymmetric vertical vorticity, the structure of the disturbances which develop in the vortex core is best seen through examination of the horizontal vorticity on a vertical slice through the center of the vortex. Contours of the y -component of vorticity on an x - z plane vertical slice are shown in Fig. 7 for the $c = 0.0$ and $c = 0.04$ simulations. For the stretched case, the size and shape of the slice has been stretched according to the evolution of the flow field, such that the two domains represent a slice of the same body of fluid. At $t = 10$, the horizontal vorticity ranges in values from 1.83 to -1.83 in the unstretched case. In the stretched case, the vorticity ranges only from 1.04 to -0.952 . This demonstrates the substantial suppression of horizontal vorticity which seems to be evident in the vortex line illustrations of Fig. 5. The variance of the vorticity field within the domain is 0.1714 in the unstretched case and only 0.0838 in the stretched case. Again, we can ask to what extent the suppression of the horizontal vorticity is due to the purely kinematic effects, and how much is due to any addi-

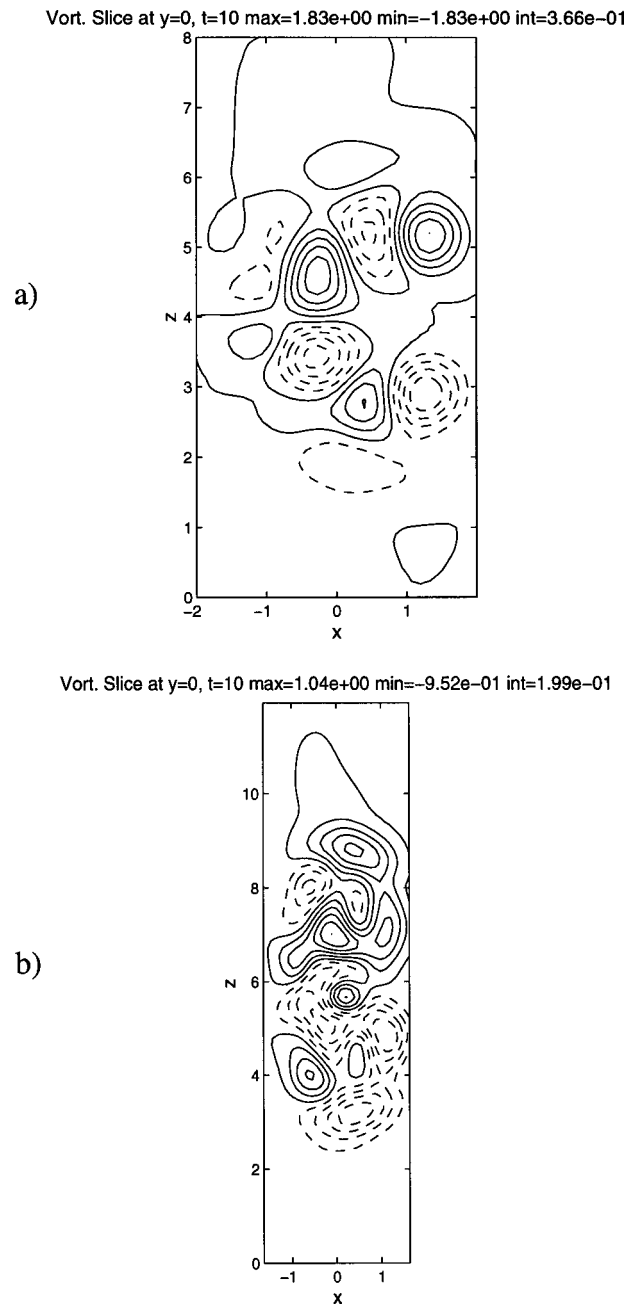


FIG. 7. Vertical cross sections in the x - z plane of the horizontal vorticity in the y direction for the stable, strongly perturbed vortex at $t = 10$ for (a) the unstretched case ($c = 0.0$); (b) the stretched case ($c = 0.04$).

tional decrease in the nonlinear dynamics. If we divide the horizontal vorticity in the stretched case by the factor $e^{-ct/2} = 0.8187$ for $c = 0.04$ and $t = 10.0$, the range of the vorticity in the stretched case would be from 1.27 to -1.16 , which is significantly smaller than the range of the vorticity in the unstretched case. The variance, renormalized by the stretching, would be 0.125. In fact, this exponential factor likely overestimates the effect of the deformation, since much of the horizontal vorticity has only recently been generated before the moment in question. The stabilization which occurs in the case of the perturbed, stable vortex is significant, and clearly larger than that expected from the kinematic effects of the deformation alone.

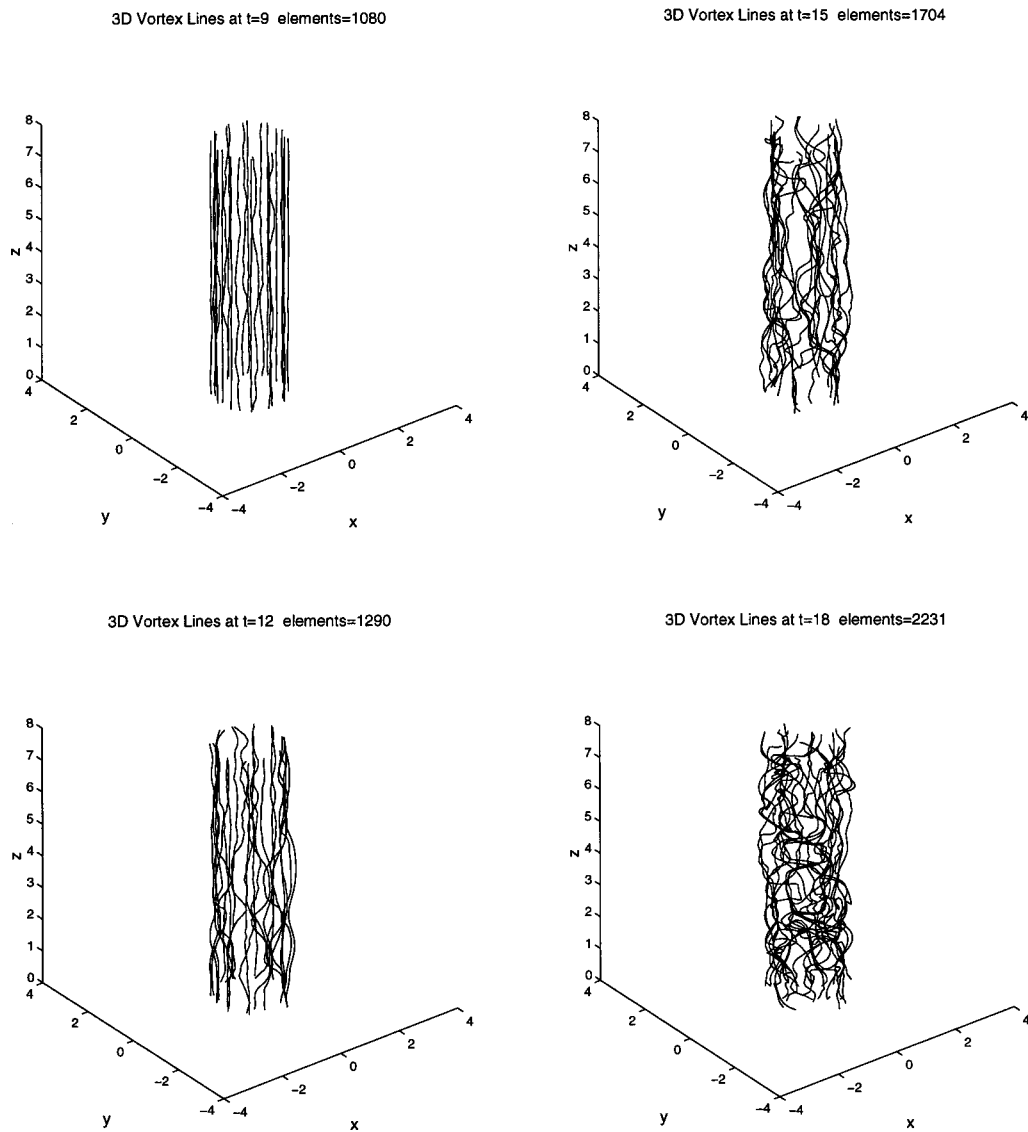


FIG. 8. Snapshots of the vortex lines for the unstable vortex at $t=9, 12, 15,$ and 18 , without axial stretching ($c=0$).

Velocity Slice at $z=4$ at $t=14$ max $[v_x, v_y]=0.70943$ max $v_z=0.050744$ interval=0.010566

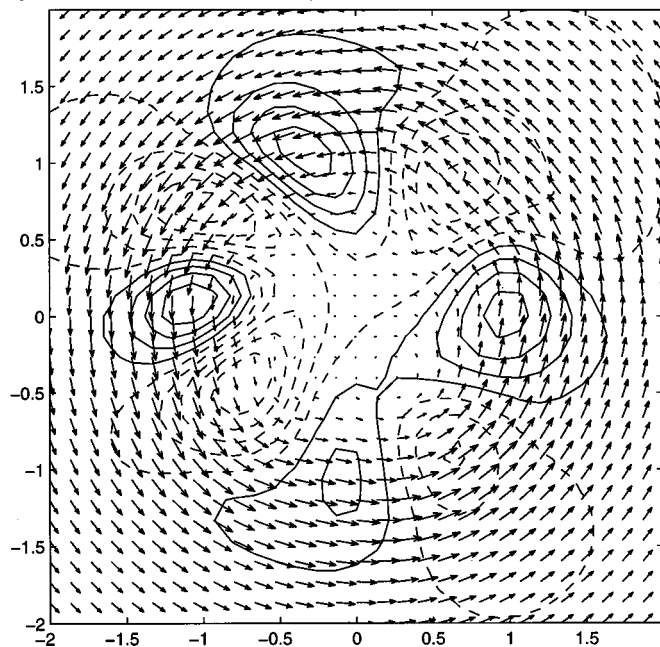


FIG. 9. Horizontal cross section of the horizontal velocity vectors and contours of the vertical velocity in the unstable vortex without deformation ($c=0.0$) at $t=14.0$.

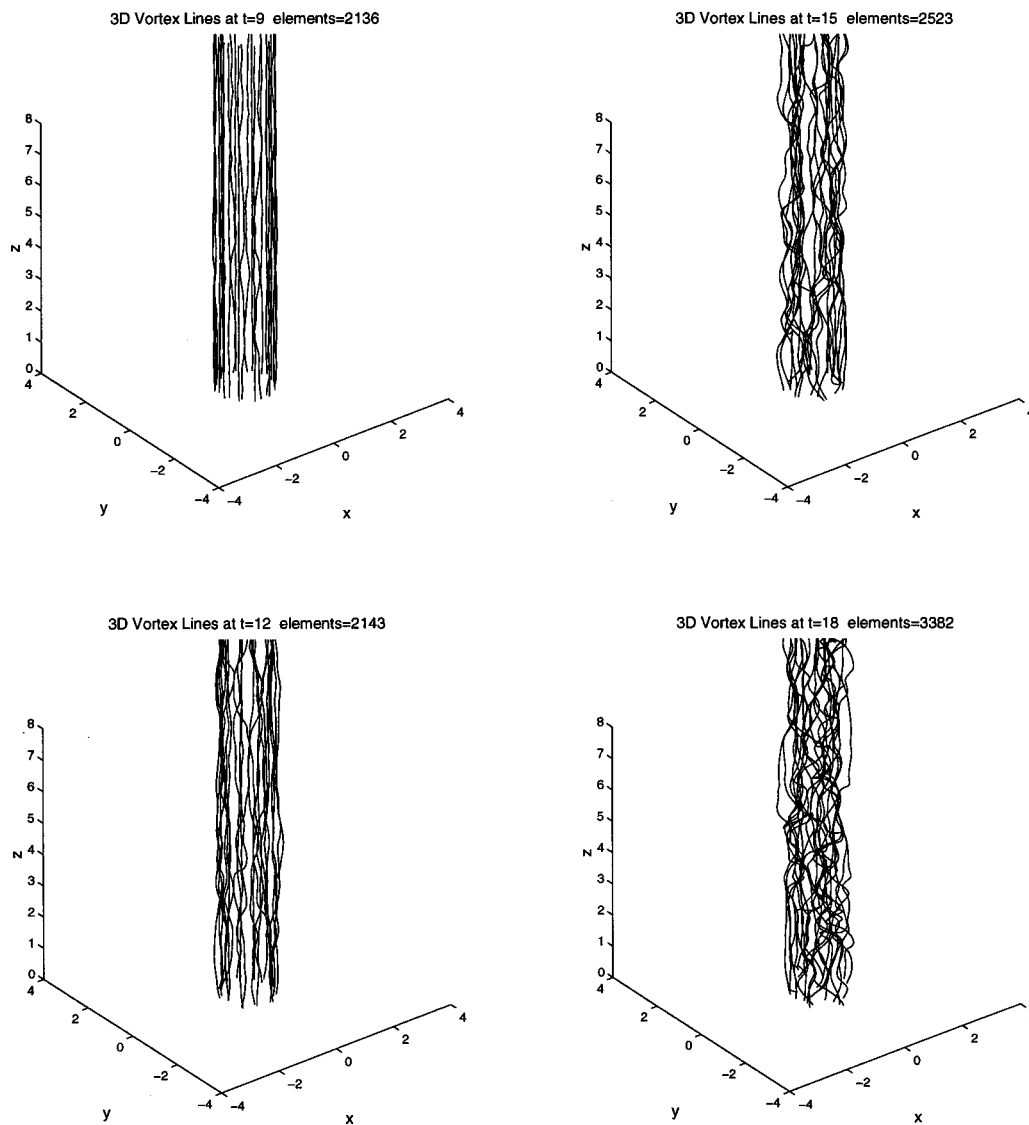


FIG. 10. Snapshots of the vortex lines for the unstable vortex at $t=9$, 12, 15, and 18, with axial stretching ($c=0.04$).

V. EVOLUTION OF THE UNSTABLE VORTEX

Snapshots of the time evolution of the vortex lines for the unstable, weakly perturbed vortex without stretching ($c=0$) are shown in Fig. 8. At early times, three-dimensional perturbations can be seen growing on the vortex lines. An interesting observation from all the unstable vortex simulations is that the vortex does not go through a period of two-dimensional instability before three-dimensional perturbations appear: It proceeds immediately to three-dimensional dynamics. (Further discussions on the issue of two-dimensional versus three-dimensional instabilities in three-dimensional vortices are available;^{38,39} however, the vortices studied in those papers are quite different from our unstable vortex.) From visual inspection, the vertical wavelengths of these disturbances appears to be comparable to the vortex radius; more precise measurements of these wavelengths will be presented below. Figure 9 shows a horizontal cross section of the horizontal velocity vectors and contours of the vertical velocity field at $t=14.0$. A wave number 4 pattern is visible, particularly in the vertical velocity field. This indi-

cates that it is not the wave number 12 pattern inherent to the initial conditions that spawns the disturbances, and that the growing wave number 4 instability is well-resolved by the 24 vortex lines.

Evolution of the same vortex under stretching with $c=0.04$ is shown in Fig. 10. The evolution appears to be quite similar to that which occurred without stretching. It does appear that the vertical wavelength of the disturbances is longer in the stretched case; compare, for example, the vortex lines at $t=12$ with and without stretching. The total modified lengths L^* of the vortex lines are shown in Fig. 11. For $c=0.02$ and $c=0.04$, the total modified length and its growth rates are in fact just slightly larger than for $c=0.0$ during the simulation. However, for $c=0.06$, there is a visible decrease in L^* and its growth rate after $t=16$. For $c=0.08$, there is a substantial decrease in L^* as compared to the other simulations.

Figure 12 shows vertical cross sections of the y -component of the vorticity field at $t=15$ for the $c=0.0$, $c=0.04$, and $c=0.08$ cases. The horizontal vorticity

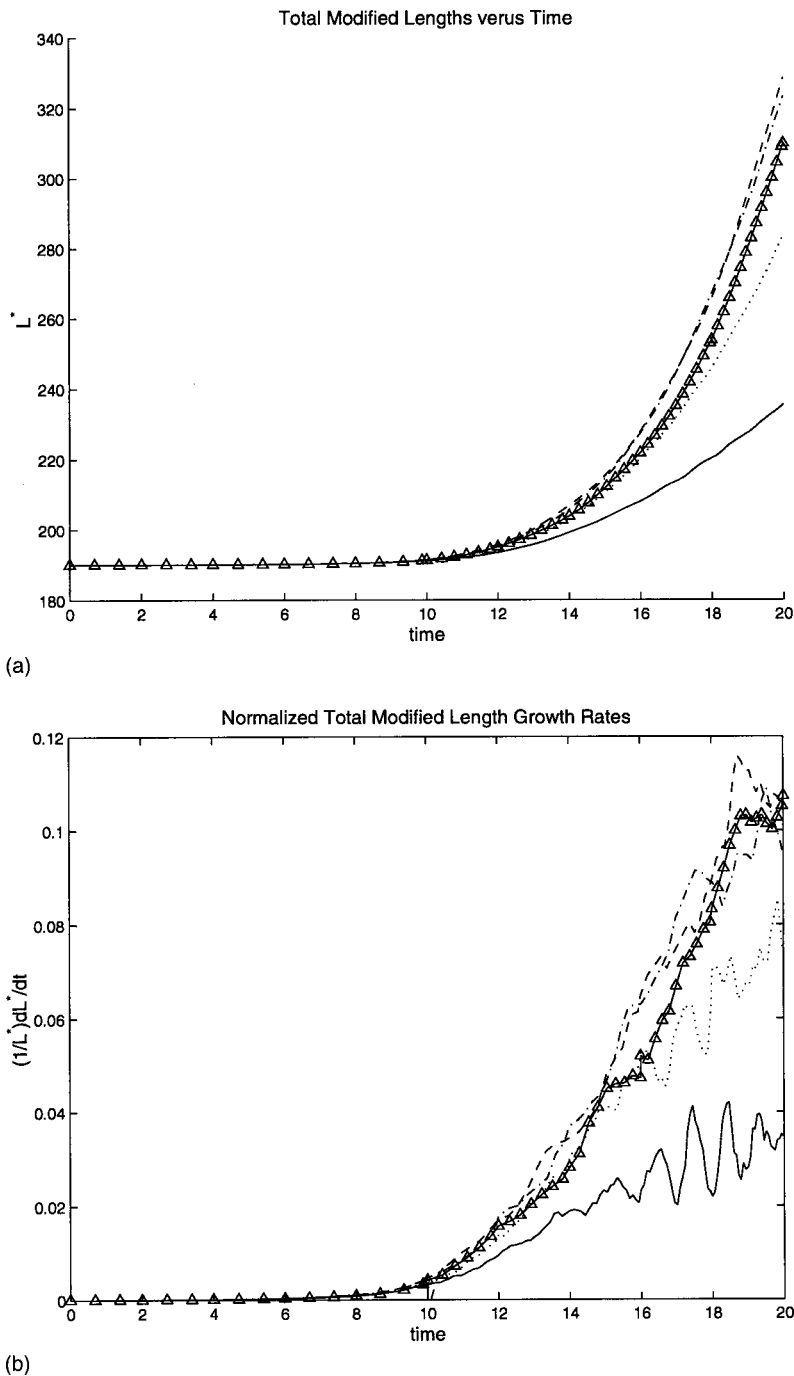


FIG. 11. Total modified lengths of the vortex lines (a) and their normalized growth rates (b), as a function of time for the unstable vortex for various values of the deformation parameter c : solid with triangles, $c=0.0$; dashed, $c=0.02$; dash-dot, $c=0.04$; dotted, $c=0.06$, and solid, $c=0.08$.

amplitudes are again decreased in the stretched vortex. The variance of the horizontal vorticity field is 1.71×10^{-2} in the unstretched vortex as compared to 7.55×10^{-3} with $c=0.04$ and 2.10×10^{-3} with $c=0.08$. Normalized by the compression factor $e^{-ct/2}$, these variance values would be 1.38×10^{-2} and 6.97×10^{-3} , respectively. As we saw in the case of the stable, perturbed vortex, the decrease in horizontal vorticity is even greater than what one would expect from the purely kinematic effects of the stretching. While the difference is small with $c=0.04$ (as the data in Fig. 12 indicate), it is substantial with $c=0.08$.

An even more direct way to quantify the growth rates and the length scales of the growing disturbances is through Fourier analysis of the paths of the vortex lines. For each

vortex line, the function $x(z)$ was first interpolated onto a higher-resolution grid on the z axis with 256 evenly spaced points using cubic splines. A Fourier transform of $x(z)$ is performed for each line, and the results were averaged for the 24 lines. The square root of the power spectrum of the mean Fourier transform of the x -displacements of the vortex lines at $t=10.0$, 11.0 , and 12.0 are shown for the simulations with $c=0.0$ and $c=0.04$ in Fig. 13; we take the square root so that the curve indicates the magnitude of the displacements at each wavelength. The results for $c=0.0$ show the rapid growth of disturbances with a vertical wavelength of 1.0. The results for $c=0.04$, shown on a plot with the same axes, also show growth of disturbances with a wavelength near 1.0, but with two important differences. First, the am-

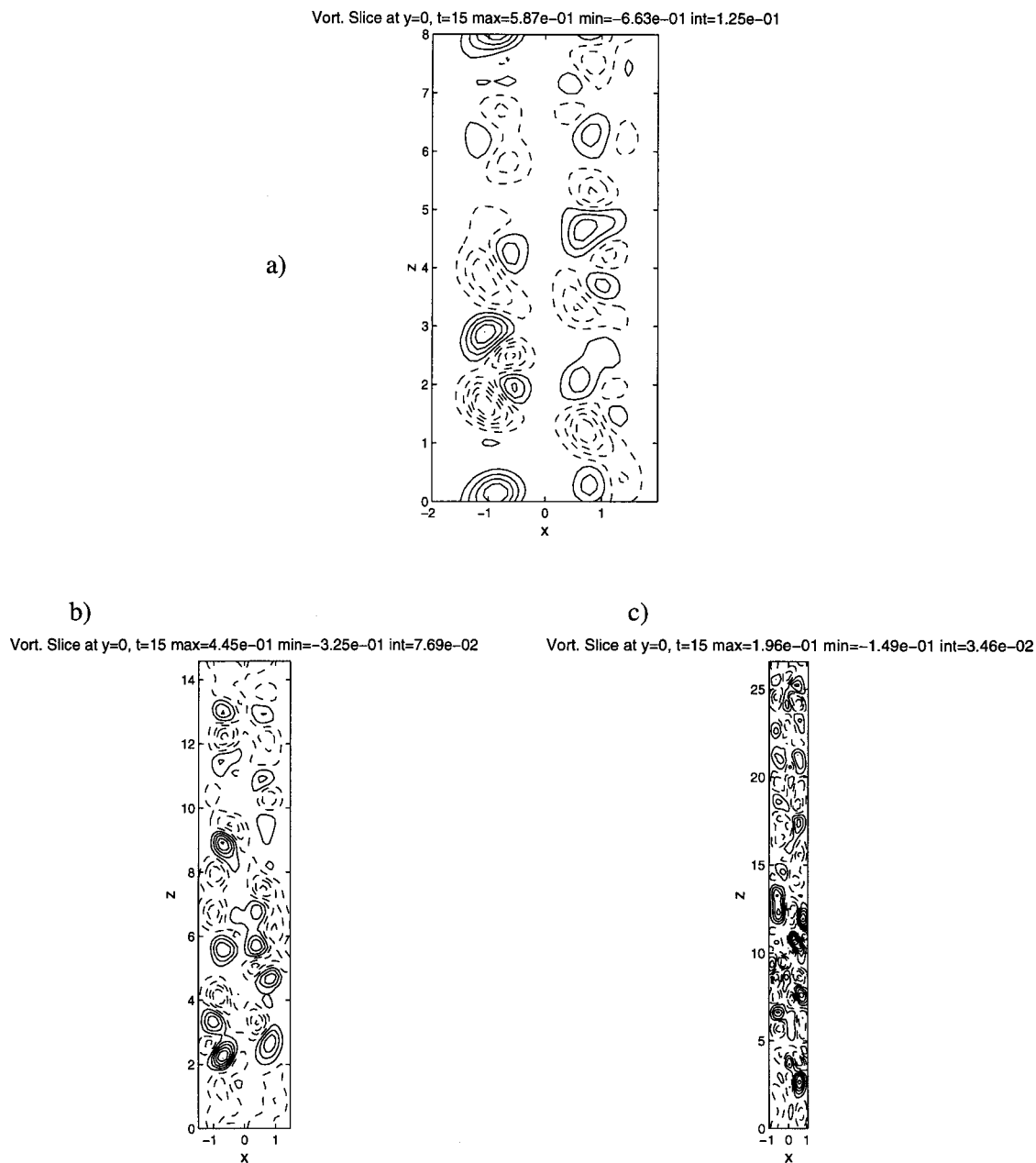


FIG. 12. Vertical cross sections in the x - z plane of the horizontal vorticity in the y direction for the unstable vortex at $t = 15$ for (a) the unstretched case ($c = 0.0$); (b) the stretched case with $c = 0.04$; (c) the stretched case with $c = 0.08$.

plitudes and growth rates of the disturbances are less; second, the wavelength of the maximum amplitude is also increasing in time.

Furthermore, we again find that the decrease in the vortex line displacements is even greater than what one would expect purely as a result of the spatial contraction associated with the deformation field. Just as points originally one unit of distance apart in the vertical direction are e^{ct} units apart at time t , points one unit apart in either the x or y directions will later be separated by a distance of $e^{-ct/2}$. In the unstretched case, the maximum displacement amplitude is 3.2×10^{-3} . If we multiply this by the factor $e^{-ct/2} = 0.7866$ for $c = 0.04$ and $t = 12.0$, we have a displacement amplitude of 2.5×10^{-3} , which is still larger than the maximum displacement amplitude in the stretched simulation. This fact is remarkable con-

sidering that the growth rate of the most unstable mode should be *increasing* in time, since the spatial contraction of the vortex core decreases the length scale while increasing the velocity scale. Even during the early growth of instabilities, the stabilizing effect of the axial stretching overwhelms the increasing instability of the vortex.

VI. DISCUSSION

The essential results are summarized in Fig. 14, which shows for both cases the normalized growth rates of the total modified lengths of the vortex lines at the end of each simulation ($t = 13.0$ for the stable, perturbed vortex and $t = 20.0$ for the unstable vortex) versus the stretching parameter c . Both the growth rates and the stretching parameter have been

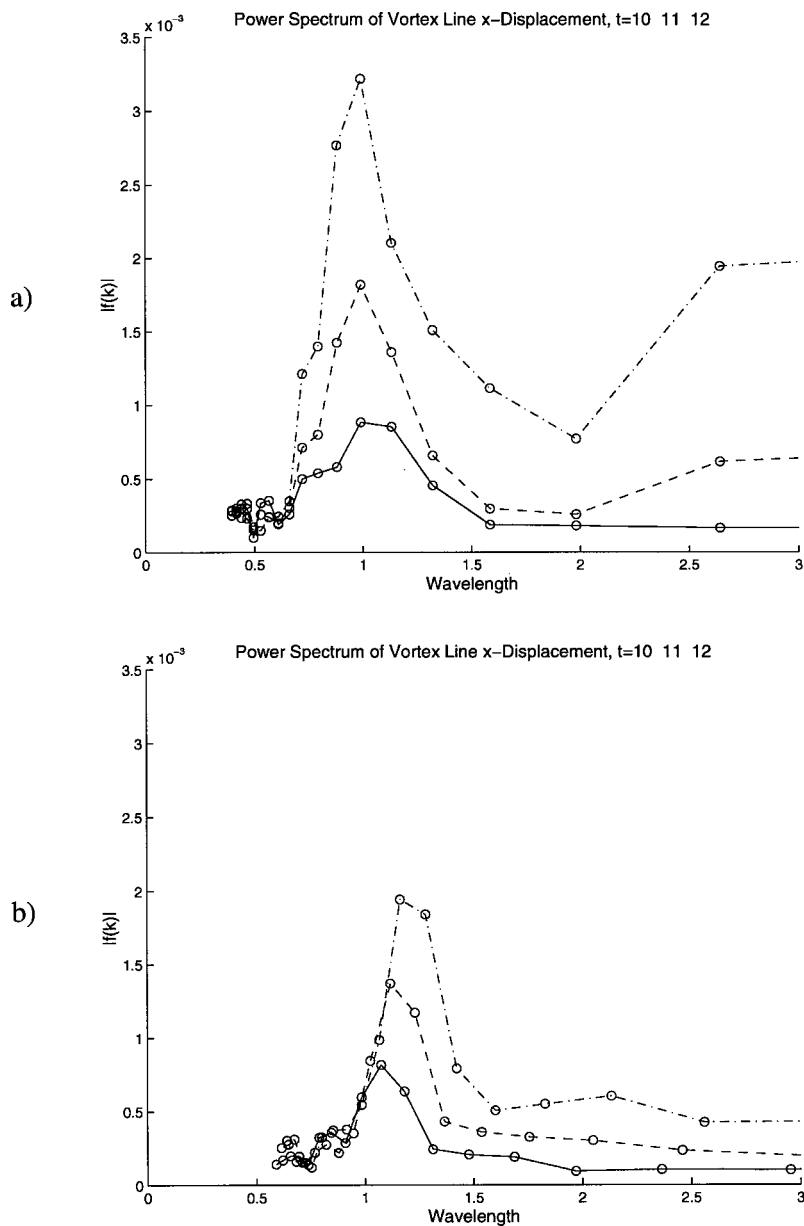


FIG. 13. Square roots of the mean power spectra of the Fourier transforms of the x -coordinate of the positions of the vortex lines in the unstable vortex, (a) without stretching ($c=0.0$); (b) with stretching ($c=0.04$). In both cases, solid lines are for $t=10.0$, dashed lines are for $t=11.0$, and dash-dot lines are for $t=12.0$.

normalized by the maximum vorticity at the start of the simulation. The growth rates steadily decline with increasing deformation; the declines of the growth rates are somewhat similar for the two cases.

There are two aspects of the stabilization by axial stretching. The kinematic effects of the deformation field are easy to understand. Any vorticity which is generated in the horizontal direction, by vortex tilting, followed by possible amplification via stretching, will experience a diminishing effect due to the contraction of the fluid along the x and y axes. In terms of the vortex lines, one can think of the deformation field as trying to "straighten" the lines back into the axial direction. The vortices we have considered here are quite unstable, such that these effects can slow, but do not stop, the transition to turbulence.

However, the stabilizing effects, and the extent to which the transition to turbulence is slowed, are even greater than what one might expect from the kinematic effects of the deformation field. This was seen for all deformation rates on

the stable, perturbed vortex, and for large deformation rates on the unstable vortex. What is the mechanism for this additional stabilization effect? The interactions of both real and numerical vortex lines are highly nonlinear, especially in regards to the self-interaction of curved vortex lines, which increases rapidly as the amount of curvature increases.⁴⁰⁻⁴⁴ (As a simple example, the self-induced motion of a thin vortex ring increases rapidly as its radius of curvature decreases.^{36,40}) Since the deformation acts to straighten the vortex lines, there is an additional negative feedback on the nonlinear vortex dynamics due to the decreased curvatures of the lines. This slows the cascade of motion and energy to smaller scales. Further study of the effects of deformation on vortex curvature and nonlinear vortex dynamics are certainly worthy of study, but are beyond the scope of this paper.

The kinematic and nonlinear mechanisms described above apply equally to both the perturbed, stable vortex and the unstable vortex. A third argument can be made which may apply only to the unstable vortex. We have observed

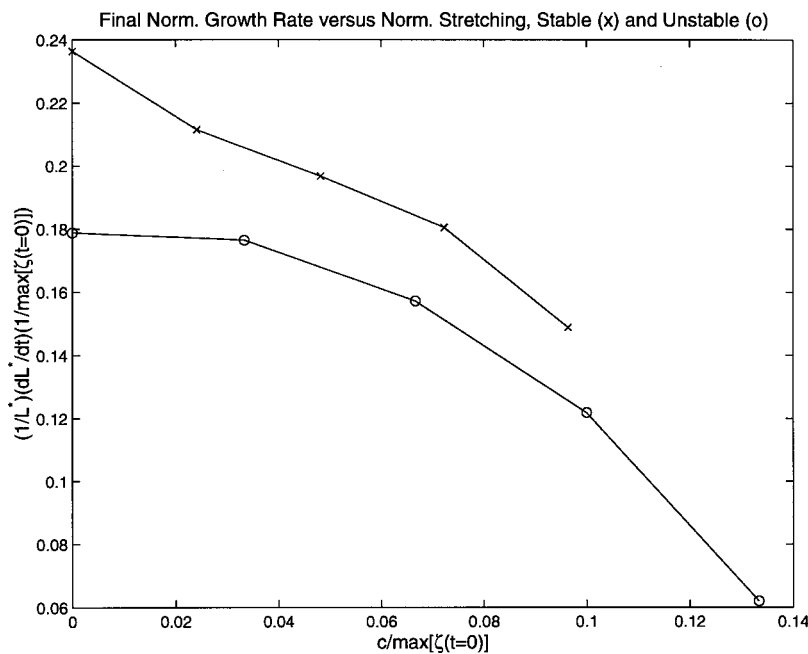


FIG. 14. Normalized growth rates of the total modified line lengths at the ends of the simulations vs the stretching intensity, for the stable, strongly perturbed vortex (o's) and the unstable vortex (x's). The growth rates and deformation rates are normalized by the maximum initial vorticity.

that the vortex proceeds immediately to three-dimensional instabilities with a vertical length scale comparable to the vortex radius. As the vortex is stretched, this radius is decreasing; however, the vertical wavelengths of the perturbations are simultaneously increasing. Thus, the stretching continuously moves the wavelengths of the perturbations away from the most unstable wavelength. This is essentially the same argument made for the stabilizing effect of stretching on elliptical, strained vortices,^{15,16} except that it applies to the large-scale modes of a fundamentally unstable vortex, rather than to the smaller-scale modes associated with the ellipticity of the flow.

VII. CONCLUSIONS

We have shown how the transition to turbulence of perturbed or unstable vortices can be slowed when the vortex is embedded in a deformation field that is aligned with the vortex axis. This stabilizing effect appears to be equally effective for both the stable, but strongly perturbed vortex and the unstable vortex, and the effect increases with increasing rates of stretching. However, in none of the simulations was the growth of perturbations or the cascade to small scales halted or reversed. Whether or not a marginally nonlinearly unstable vortex can be completely stabilized by stretching remains for future work.

Although these results have significant implications for vortices maintained by deformation (stretching), further study is warranted before our conclusions can be applied unconditionally to atmospheric vortices. There are a number of important distinctions between the vortices simulated in this study and tornadoes, mesocyclones, and hurricanes. Our vortices are not in a steady state, but rather are continuously contracting in scale. To achieve a steady state, diffusion (molecular or turbulent) must be incorporated. The best-studied method for simulating diffusion in two- and three-dimensional vortex methods involves adding a random walk

to the paths of the vortex elements.^{19,20,45,46} This method is highly problematic in three dimensions because it rapidly increases the complexity of the vortex lines; while the vorticity field is effectively smoothed by this approach, the number of elements increases rapidly and the simulation quickly becomes computationally unfeasible. However, the recent development of "deterministic" diffusion methods,⁴⁷ particularly the concept of a "diffusion velocity,"⁴⁸ will hopefully allow for viscous three-dimensional vortex method simulations in the near future.

Furthermore, the deformation fields which sustain intense vortices in the atmosphere are not nearly so geometrically simple as the unbounded, axisymmetric deformation field used in this study. In particular, the secondary circulations associated with both tornadoes and hurricanes have weak radial inflow without vertical stretching outside of the vortex core, while the almost all the vertical motion and stretching are confined to an annulus near and around the radius of maximum winds. While stabilizing effects have been observed for linearized, two-dimensional perturbations in idealized vortices with spatially varying deformation,^{14,49} further work remains for more realistic, three-dimensional flows.

The results of this study may be much more applicable to the real atmosphere if we change our point of view. On small scales most intense atmospheric vortices are highly turbulent. As (relatively) small parcels of fluid are carried into the vortex core and then rapidly advected up from the surface, they will undergo considerable deformation much more like the type used in this study. While the stabilizing effect of stretching remains in question for the vortex as a whole, perhaps individual parcels of air in the vortex core will feel this effect, leading to a decrease in the intensity of turbulence in the vortex core.

In light of the close connection between the stability of stretched vortices and the three-dimensional instabilities of

vortices subjected to planar strain,^{11–13,15–18} a study of three-dimensional vortex dynamics under planar strain, with and without axial stretching also present, would be a natural extension of this work. Since a planar strain flow also has zero vorticity, it could be incorporated into the three-dimensional vortex methods framework just as easily as the axisymmetric stretching field. This will be the subject of future work.

ACKNOWLEDGMENTS

The author would like to thank A. Chorin for many helpful discussions and D. Adalsteinsson for extensive programming and visualization guidance. An anonymous reviewer provided some helpful suggestions and pointed the way some very significant references. This work was supported by the Applied Mathematical Sciences Subprogram of the Office of Energy Research, U.S. Department of Energy under Contract No. DE-AC03-76SF-00098, by the Office of Naval Research under Contract No. N00014-93-1-0456 P00006, and by Colorado State University.

- ¹J. B. Klemp, "Dynamics of tornadic thunderstorms," *Annu. Rev. Fluid Mech.* **19**, 362 (1987).
- ²R. Rotunno, "Supercell modelling and theory," *The Tornado: Its Structure, Dynamics, Precipitation, and Hazards*, edited by C. Church *et al.* (American Geophysical Union, Washington, D.C., 1993), pp. 57–73.
- ³R. A. Anthes, *Tropical Cyclones: Their Evolution, Structure, and Effects*, Meteorol. Monogr. No. 41 (American Meteorological Society, Boston, 1982), p. 298.
- ⁴D. W. Moore and P. G. Saffman, "The instability of a straight vortex filament in a strain field," *Proc. R. Soc. London, Ser. A* **346**, 413 (1975).
- ⁵C.-Y. Tsai and S. E. Widnall, "The stability of short waves on a straight vortex filament in a weak externally imposed strain field," *J. Fluid Mech.* **73**, 721 (1976).
- ⁶A. C. Robinson and P. G. Saffman, "Three dimensional stability of an elliptical vortex in a straining field," *J. Fluid Mech.* **142**, 451 (1984).
- ⁷R. T. Pierrehumbert, "Universal short-wave instability of two-dimensional eddies in an inviscid fluid," *Phys. Rev. Lett.* **57**, 2157 (1986).
- ⁸M. J. Landman and P. G. Saffman, "The three-dimensional instability of strained vortices in a viscous fluid," *Phys. Fluids* **30**, 2339 (1987).
- ⁹F. Waleffe, "On the three-dimensional instability of strained vortices," *Phys. Fluids A* **2**, 76 (1990).
- ¹⁰J. M. Burgers, "A mathematical model illustrating the theory of turbulence," *Adv. Appl. Mech.* **1**, 197 (1948).
- ¹¹A. C. Robinson and P. G. Saffman, "Stability and structure of stretched vortices," *Stud. Appl. Math.* **70**, 163 (1984).
- ¹²H. K. Moffat, S. Kida, and K. Ohkitani, "Stretched vortices—the sinews of turbulence; large Reynolds number asymptotics," *J. Fluid Mech.* **259**, 241 (1994).
- ¹³A. Prochazka and D. I. Pullin, "Structure and stability of non-symmetric Burgers vortices," *J. Fluid Mech.* **363**, 199 (1998).
- ¹⁴D. S. Nolan and B. F. Farrell, "Generalized stability analyses of asymmetric disturbances in one- and two-celled vortices maintained by radial inflow," *J. Atmos. Sci.* **56**, 1282 (1999).
- ¹⁵S. Le Dizès, M. Rossi, and H. K. Moffatt, "On the three-dimensional instability of elliptical vortex subjected to stretching," *Phys. Fluids* **8**, 2084 (1997).
- ¹⁶C. Eloy and S. Le Dizès, "Three-dimensional instability of Burgers and Lamb–Oseen vortices in a strain field," *J. Fluid Mech.* **378**, 145 (1999).
- ¹⁷J. C. Neu, "The dynamics of stretched vortices," *J. Fluid Mech.* **143**, 253 (1984).
- ¹⁸R. Klein, A. J. Majda, and R. M. McLaughlin, "Asymptotic equations for the stretching of vortex filaments in a background flow field," *Phys. Fluids A* **4**, 2271 (1992).
- ¹⁹A. J. Chorin, "Numerical study of slightly viscous flow," *J. Fluid Mech.* **57**, 785 (1973).
- ²⁰A. J. Chorin, "Vortex methods," *Computational Fluid Dynamics*, edited by M. Lesieur *et al.* (Elsevier, New York, 1996).
- ²¹E. G. Puckett, "Vortex methods: An introduction and survey of selected research topics," *Incompressible Computational Fluid Dynamics—Trends and Advances*, edited by M. D. Gunzburger and A. A. Nicolaides (Cambridge University Press, Cambridge, 1993).
- ²²J. T. Beale and A. J. Majda, "Vortex methods II: Higher order accuracy in two and three space dimensions," *Math. Comput.* **32**, 29 (1982).
- ²³J. T. Beale and A. Majda, "High order accurate vortex methods with explicit velocity kernels," *J. Comput. Phys.* **58**, 188 (1985).
- ²⁴O. H. Hald, "Convergence of vortex methods for Euler's equations, II," *SIAM (Soc. Ind. Appl. Math.) J. Numer. Anal.* **16**, 726 (1979).
- ²⁵O. H. Hald, "Convergence of vortex methods for Euler's equations, III," *SIAM (Soc. Ind. Appl. Math.) J. Numer. Anal.* **24**, 538 (1987).
- ²⁶A. J. Chorin, "The evolution of a turbulent vortex," *Commun. Math. Phys.* **83**, 517 (1982).
- ²⁷A. Leonard, "Computing three-dimensional incompressible flows with vortex filaments," *Annu. Rev. Fluid Mech.* **17**, 523 (1985).
- ²⁸O. M. Knio and A. F. Ghoniem, "Three dimensional vortex methods," *J. Comput. Phys.* **86**, 75 (1990).
- ²⁹In preliminary work by the author [D. S. Nolan, "Vortex stabilization in deformation fields," *12th Conference on Atmospheric and Oceanic Fluid Dynamics*, New York City, June, 1999 (American Meteorological Society, Boston, MA, 1999), pp. 290–293] a different core function presented by Beale and Majda (see Ref. 23) was used which is known to allow for fourth-order convergence. However, this core function has negative vorticity making the construction of single-signed vorticity fields rather difficult.
- ³⁰For particle (and vortex) methods, the order refers to the rate of accuracy increase as the number of particles is increased.
- ³¹H. Y. Wang, "A study of short wave instability on vortex filaments," Ph.D. Thesis, Department of Mathematics, U.C. Berkeley, 1996.
- ³²O. M. Knio and A. F. Ghoniem, "Three dimensional vortex simulation of rollup and entrainment in a shear layer," *J. Comput. Phys.* **97**, 172 (1991).
- ³³J.-C. J. Saghbini and A. F. Ghoniem, "Numerical simulation of the dynamics and mixing in a swirling flow," *Proceedings, 35th Aerospace Sciences Meeting and Exhibit* (American Institute of Aeronautics and Astronautics, Reston, VA, 1997).
- ³⁴Alternatively, one can think of the axisymmetric deformation field as a flow induced by infinitely strong vortex rings infinitely far away.
- ³⁵Lord Kelvin, "Vibrations of a columnar vortex," *Philos. Mag.* **10**, 155 (1880).
- ³⁶P. G. Saffman, *Vortex Dynamics* (Cambridge University Press, Cambridge, 1992), pp. 215–218.
- ³⁷The author would like to thank Prof. A. Majda for this observation.
- ³⁸P. R. Gent and J. C. McWilliams, "The instability of barotropic circular vortices," *Geophys. Astrophys. Fluid Dyn.* **35**, 209 (1986).
- ³⁹W. D. Smyth and J. C. McWilliams, "Instability of an axisymmetric vortex in a stably stratified, rotating environment," *Theor. Comput. Fluid Dyn.* **11**, 305 (1998).
- ⁴⁰G. K. Batchelor, *An Introduction to Fluid Mechanics* (Cambridge University Press, Cambridge, 1967).
- ⁴¹H. Hasimoto, "A soliton on a vortex filament," *J. Fluid Mech.* **51**, 477 (1972).
- ⁴²R. Klein and A. Majda, "Self stretching of a perturbed vortex filament I. The asymptotic equations for deviations from a straight line," *Physica D* **49**, 323 (1991).
- ⁴³R. Klein and A. Majda, "Self stretching of a perturbed vortex filament II. Structure of solutions," *Physica D* **53**, 267 (1991).
- ⁴⁴R. Klein and O. M. Knio, "Asymptotic vorticity structure and numerical simulation of slender vortex filaments," *J. Fluid Mech.* **284**, 275 (1995).
- ⁴⁵J. Goodman, "The convergence of random vortex methods," *Commun. Pure Appl. Math.* **40**, 189 (1987).
- ⁴⁶D. G. Long, "Convergence of the random vortex method in two dimensions," *J. Am. Math. Soc.* **1**, 779 (1988).
- ⁴⁷D. Fishelov, "A new vortex scheme for viscous flows," *J. Comput. Phys.* **86**, 211 (1990).
- ⁴⁸E. Rivoalen and S. Huberson, "Numerical simulation of axisymmetric viscous flows by means of a particle method," *J. Comput. Phys.* **152**, 1 (1999).
- ⁴⁹D. S. Nolan and B. F. Farrell, "The intensification of two-dimensional swirling flows by stochastic asymmetric forcing," *J. Atmos. Sci.* **56**, 3937 (1999).